

A Faceted Prior for Scalable Wideband Imaging: Application to Radio Astronomy

P.-A. Thouvenin[§], A. Abdulaziz^{*}, M. Jiang[†], A. Repetti^{‡*}, A. Dabbech^{*} and Y. Wiaux^{*}

[§] Université de Lille, CNRS, Centrale Lille, UMR 9189 CRIStAL, F-59000 Lille, France

^{*}Institute of Sensors, Signals and Systems, Heriot-Watt University, Edinburgh EH14 4AS, United Kingdom

[†]Signal Processing Laboratory 5, École Polytechnique Fédérale de Lausanne, CH-1015, Lausanne, Switzerland

[‡]Department of Actuarial Mathematics & Statistics, Heriot-Watt University, Edinburgh EH14 4AS, United Kingdom.

1. Context and proposed approach

- Objective:** form extreme size wideband image \mathbf{X} from incomplete data

$$\begin{bmatrix} \mathbf{Y} \\ \vdots \\ \mathbf{Y} \end{bmatrix} = \Phi \begin{pmatrix} \mathbf{X} \\ \vdots \\ \mathbf{X} \end{pmatrix} + \mathbf{N}, \quad \bar{\mathbf{X}} \in \mathbb{R}^{N \times L}, \quad \mathbf{Y}, \mathbf{N} \in \mathbb{C}^{M \times L}$$

$$\rightsquigarrow \text{optimization problem: } \underset{\mathbf{X} \in \mathbb{R}_{+}^{N \times L}}{\text{minimize}} \underbrace{f(\mathbf{Y}, \Phi(\mathbf{X}))}_{\text{data fitting}} + \underbrace{r(\mathbf{X})}_{\text{regularization}}$$

- Spectral correlations: low-rankness and joint-sparsity regularization

$$r(\mathbf{X}) = \lambda \|\mathbf{X}\|_{*,\omega} + \mu \|\Psi^\dagger \mathbf{X}\|_{2,1,\bar{\omega}}, \quad \Psi^\dagger \in \mathbb{R}^{R \times N} \text{ sparsifying dictionary}$$

\rightsquigarrow [prohibitive cost]: radio-astronomy, $L \approx 10^3$ channels, $N \approx 10^{14}$ pixels

- Proposed approach:** facet-based low-rankness and joint sparsity prior

$$r(\mathbf{X}) = \sum_{q=1}^Q \lambda_q \|\mathbf{W}_q \tilde{\mathbf{S}}_q \mathbf{X}\|_{*,\omega_q} + \mu_q \|\Psi_q^\dagger \mathbf{S}_q \mathbf{X}\|_{2,1,\bar{\omega}_q}$$

\rightsquigarrow define dictionary Ψ_q^\dagger based on the structure of Ψ^\dagger ;
(exact decomposition when Ψ^\dagger is a wavelet dictionary [1])
 \rightsquigarrow [more scalable, promotes local spectral correlations];
 \rightsquigarrow $\mathbf{S}_q, \tilde{\mathbf{S}}_q$ selection operators, weights \mathbf{W}_q to mitigate faceting artifacts.

2. Application to radio-astronomy

- Measurement operator:**

$$\Phi(\mathbf{X}) = (\Phi_{b,l} \mathbf{x}_l)_{1 \leq l \leq L, 1 \leq b \leq B}, \quad \Phi_{b,l} = \Theta_{b,l} \mathbf{G}_{b,l} \mathbf{F} \mathbf{Z}$$

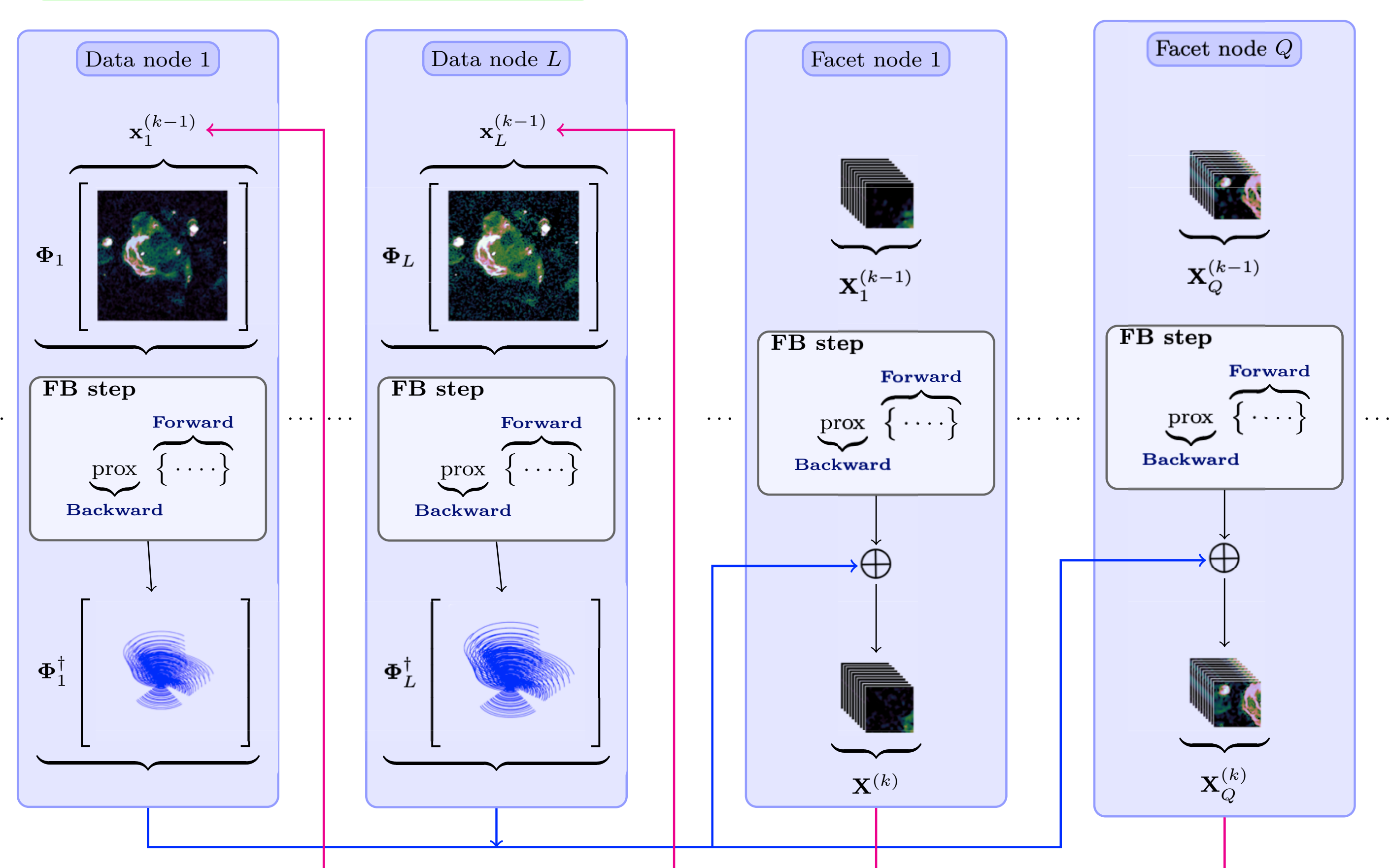
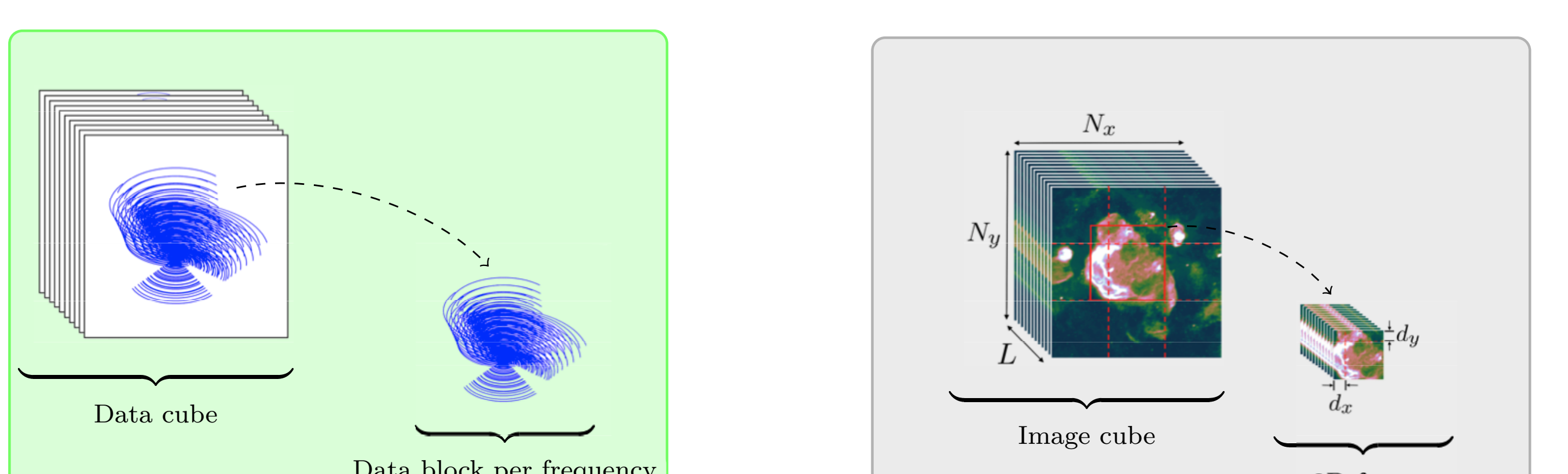
$\mathbf{x}_l \in \mathbb{R}^N$ image in channel l (column of \mathbf{X})
 $\mathbf{F} \in \mathbb{C}^{K \times K}$ Fourier transform
 $\mathbf{Z} \in \mathbb{R}^{K \times N}$ zero-padding and scaling operator
 $\Theta_{b,l} \in \mathbb{R}^{M_{b,l} \times M_{b,l}}$ natural weighting matrix (data block b , channel l)
 $\mathbf{G}_{b,l} \in \mathbb{C}^{M_{b,l} \times K}$ interpolation and calibration kernels

- Problem formulation:** extension of HyperSARA [2] – a wideband radio-interferometric (RI) imaging approach

\rightsquigarrow data fidelity: per block & channel ℓ_2 constraint, controlled by $\varepsilon_{b,l}$

$$\underset{\mathbf{X} \in \mathbb{R}_{+}^{N \times L}}{\text{minimize}} \underbrace{\sum_{l,b} \iota_{\mathcal{B}(\mathbf{y}_{b,l}, \varepsilon_{b,l})}(\Phi_{b,l} \mathbf{x}_l)}_{f(\mathbf{Y}, \Phi(\mathbf{X}))} + \underbrace{\sum_{q=1}^Q \|\mathbf{W}_q \tilde{\mathbf{S}}_q \mathbf{X}\|_{*,\omega_q} + \mu_q \|\Psi_q^\dagger \mathbf{S}_q \mathbf{X}\|_{2,1,\bar{\omega}_q}}_{r(\mathbf{X})}$$

- Imaging algorithm:** preconditioned primal-dual algorithm [3].



3. Illustration on synthetic data

- Simulation settings:**

- synthetic wideband image of the W28 supernova remnant;
 - $L = 20$ channels, $N = 1024 \times 1024$ pixels, $M \approx 0.5N$, SNR = 60 dB;
 - faceted HyperSARA compared to HyperSARA [2] and single channel reconstruction (SARA [4]):
- \triangleright quality comparable to HyperSARA, much lower computing time;
- \triangleright overall reconstruction improvement of very low intensity emissions;
- \triangleright limited performance of SARA: single channel \rightsquigarrow limited range of spatial frequencies exploited (nature of RI Fourier sampling).

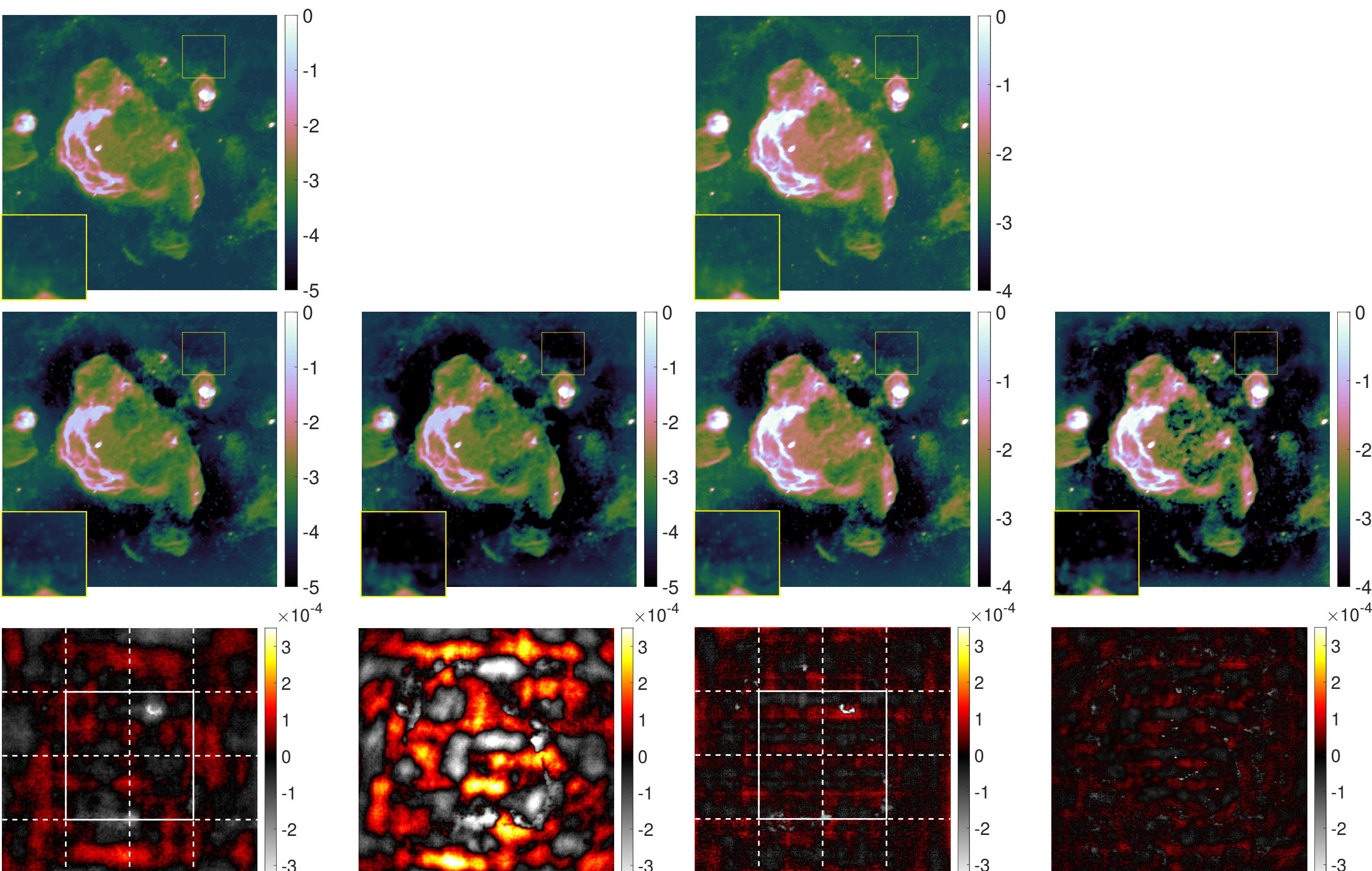


Figure 1: Results for the channel 1 (first two columns) and 20 (last two columns) for the faceted (column 1 and 3, overlap of 50%) and standard HyperSARA (column 2 and 4). From top to bottom: ground truth, reconstructed and residual images (facets delineated in white).

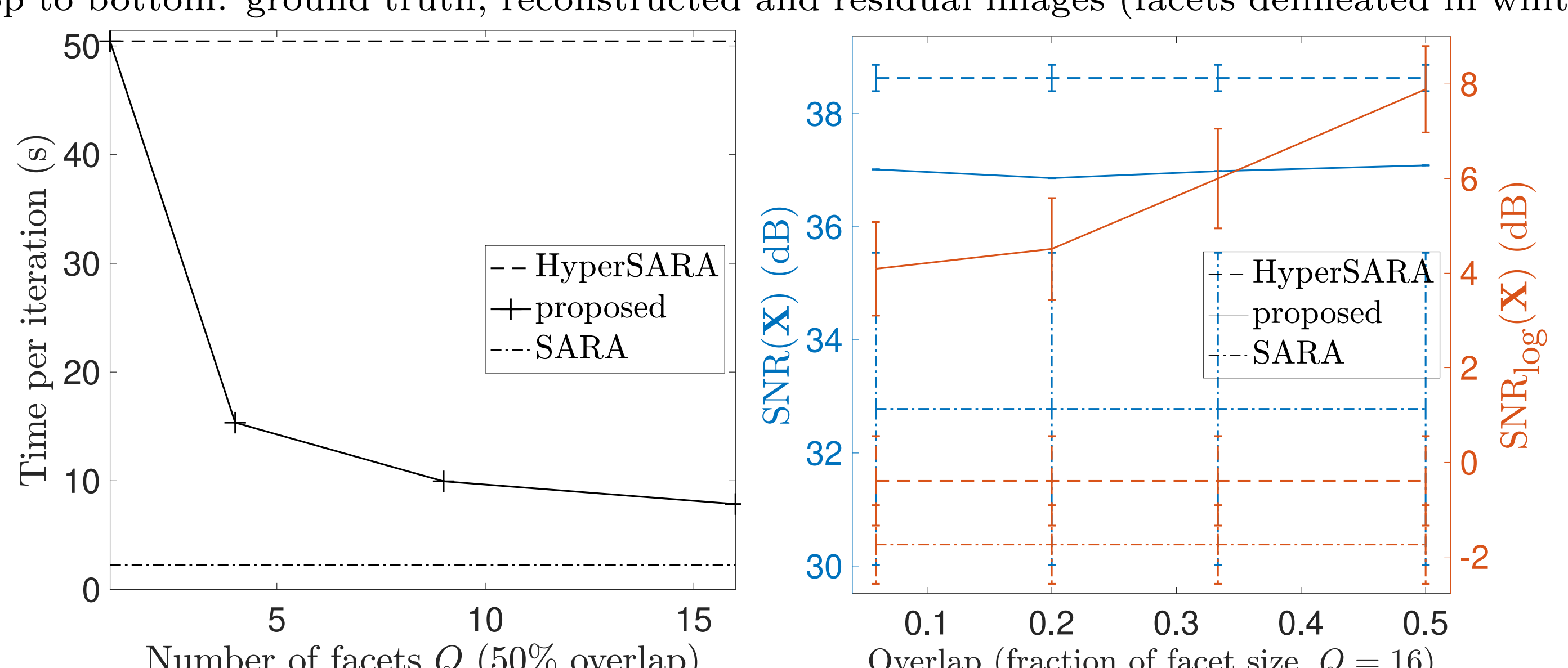


Figure 2: Computing time vs. number of facets (overlap of 50% overlap), and average SNR (SNR , SNR_{\log}) vs. overlap (error bars: ± 1 standard deviation computed over the channels).

4. Conclusions and perspectives

- Conclusions:**

- ✓ [faceted prior for scalable wideband imaging];
- ✓ [promote local spectral correlations] via a facet-based nuclear norm
 \rightsquigarrow better recovery of faint emissions compared to HyperSARA.

- Future work:**

- scalability: 16 GB proof of concept image reconstruction of Cygnus A;
- Production HPC code: C++ version of Puri-Psi software (<https://basp-group.github.io/Puri-Psi/>)

Supported in part by EPSRC grants EP/M011089/1, EP/M008843/1, EP/M019306/1, the Swiss-South Africa Joint Research Program (IZLSZ2_170863/1). Work using the Cirrus UK National Tier-2 HPC Service at EPCC (<http://www.cirrus.ac.uk>) funded by the University of Edinburgh and EPSRC (EP/P020267/1).

- [1] Z. Prusa, "Segmentwise discrete wavelet transform," PhD thesis, Brno university of technology, 2012.
- [2] A. Abdulaziz, A. Dabbech, and Y. Wiaux, "Wideband super-resolution imaging in radio interferometry via low rankness and joint average sparsity models (HyperSARA)," 2018, submitted.
- [3] J.-C. Pesquet and A. Repetti, "A class of randomized primal-dual algorithms for distributed optimization," *Journal of nonlinear and convex analysis*, vol. 16, no. 12, pp. 2453–2490, 2015.
- [4] R. E. Carrillo, J. D. McEwen, and Y. Wiaux, "Sparsity Averaging Reweighted Analysis (SARA): A novel algorithm for radio-interferometric imaging," *Monthly Notices of the Royal Astronomical Society*, vol. 426, no. 2, pp. 1223–1234, 2012.